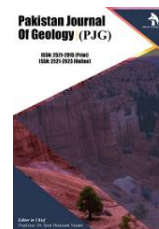


ZIBELINE INTERNATIONAL™
PUBLISHING

ISSN: 2521-2915 (Print)

ISSN: 2521-2923 (Online)

CODEN: PJGABN



RESEARCH ARTICLE

THERMAL AND BURIAL HISTORIES OF NORTHERN DEPOBELT IN THE NIGER DELTA NIGERIA USING WELL-LOG DATA

Miuweme, T. U^a, Uko, E. D^a, Amakiri, A. R. C^a, Oki, A. O^b.^aDepartment of Physics, Rivers State University, PMB 5080, Port Harcourt, Nigeria;^bDepartment of Geology, Niger Delta University, Amassoma, Bayelsa State, Nigeria.^{*}Corresponding Author Email: e_uko@yahoo.com (E. Uko)

This is an open access article distributed under the Creative Commons

Attribution License CC BY 4.0, which permits unrestricted use, distribution, and reproduction in any medium, provided the original work is properly cited.

ARTICLE DETAILS

Article History:

Received 15 July 2023

Revised 18 August 2023

Accepted 22 September 2023

Available online 28 September 2023

ABSTRACT

Well-log data from four wells located in Northern Depobelt in the Niger Delta were used for the interpretation of Thermal properties, burial history, and subsidence rate, using Petromod and Excel softwares. The geothermal gradients in wells -1, -2, -3 and -4 are 1.247°C/100m, 1.792°C/100m, 2.232°C/100m and 1.862°C/100m respectively, based on an average surface temperature of 27°C. The average geothermal gradient 1.767°C/100m for the field of study. Thermal conductivity values were highly variable with depth with values of 2.36Wm⁻¹K⁻¹, 2.27Wm⁻¹K⁻¹, 2.35Wm⁻¹K⁻¹, and 2.55Wm⁻¹K⁻¹ for Wells 1, 2, 3 and 4 respectively. The heat flux obtained for the wells are accordingly 30.73mWm⁻², 40.57mWm⁻², 50.53mWm⁻², and 42.19mWm⁻². There was the general trend of the massive sandstones in the upper layers, characteristics of the Benin formation into an alternation of both sandstone and shales characteristic of the Agbada formation, followed by an increase in shale percentage down the series. The bottom of the Benin/top of Agbada boundaries for the four wells are about 1524.0m, 1066.8m, 1981.2m and 1371.6m for Wells 1, 2, 3 and 4 respectively. The burial gradient decreases with age. Rapid subsidence episode took place between the Middle Pliocene at 3.5Ma which lasted till the Early-Pleistocene creating accommodation for the deposition of sediments with an average thickness of 1066.57m.

KEYWORDS

Burial history, temperature gradient, heatflow, well logs, Northern depobelt, Niger Delta, Nigeria.

1. INTRODUCTION

Sedimentary basins are the primary locations on the continents where sufficient subsidence exists for long-term preservation of continental sediments, and in fact may be the only locations where significant long-term preservation is possible (Weissmann, 2015). Subsidence is the downward movement of the earth's surface in response to loading by sediments, tectonic forces or land sediment compaction (Utkelbayev, 1974; Scalter et al., 1980). Subsidence depends upon the balance between the rate sedimentation and the rate of subsidence (Evamy et al., 1976).

The main objectives of this work are to investigate burial history and rate of subsidence in the area of study by constructing the subsidence curves through geologic time. The significance of this study are therefore, to provide information: to understand better the evolution of the Niger Delta

basin; on the degree of maturation of organic matter within the sediment of the Niger Delta basin; and on the palaeotemperature of sedimentary layers.

2. AREA OF STUDY AND ITS GEOLOGY

The area of study is situated in the northern part of the Niger Delta which extends from about longitude 5°30' - 6°30' East (Figure 1). The Niger Delta is located at the southern end of Nigeria which is situated on the Gulf of Guinea on the west of Central Africa. It extends from about longitude 3°E to 9°E and latitudes 4°30'N to 5°30' N. During the Tertiary period, it built out into the Atlantic Ocean at the mouth of the Niger- Benue River system on the south and is bounded on the west by the Benin Flank, on the north by the Anambra Embankment and the Abakalili Anticlinorium, while on the east by the Calabar Flank.

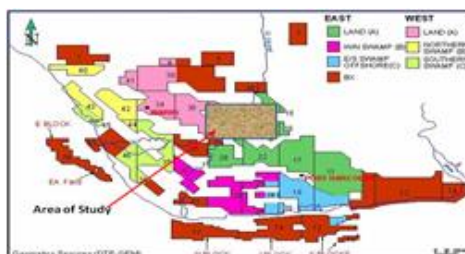


Figure 1: Map of the Niger Delta showing the area of study

The Niger Delta has an area of catchment that encompasses more than a million square kilometres of predominantly Savannah covered lowland

(Doust and Omatosola, 1990). Although the rifting stage of the Nigeria margin started in the late Jurassic, the breakup of the Africa from South

Quick Response Code



Access this article online

Website:

www.pakjgeology.com

DOI:

10.26480/pjg.01.2023.21.31

America part of Gondwanaland took place in the Mesozoic. The break-up took place along series of zones of different orientations that met in a triple junction in an area of the present Gulf of Guinea in the position now occupied by Niger Delta. Two of this arm followed the south eastern part of Nigeria and Cameroon, and developed in to the Benue Trough.

During the rift-fill phase, the first sediments of the Cretaceous to Tertiary cycle accumulated, the oldest of these have been dated Albian. Thick succession of marine and marginal marine classics and carbonates were deposited in a series of transgressive and regressive phase. This rift-fill phase ended with a basin inversion, with possible change related to the restriction of movement of the Africa plate due to the first Alpine tectonic phases. Renewed subsidence occurred as the continent completely separated, and the sea transgressed as far inland as the Benue Trough. The youngest Cretaceous sediments deposited during this early drift phase comprise classics, mainly of a regressive deltaic series. This formed a proto-Niger Delta which built out over the collapsed continental margin, and has its core located above the collapsed continental margin at the side of the triple junction. Initially, the delta prograded over extensionally thinned and collapsed continental crust of the West Africa margin as far as the triple junction, filling in the basement graden-and-horst topography. The convex-to-sea morphology did not develop until Eocene.

Regression has been rapid since then and increasing volumes of sediments have been deposited since the Oligocene. The growth of the Tertiary Niger Delta however, can be depicted by a series of maps showing the principal depocentres for selected micro-floral units between the Paleocene and Pliocene. One striking feature of the present day Delta is the sandy nature of the sediment. This is partly as a result of the fact that, nearly the entire environment in the sub-aerial is of upper coastal or delta plain origin. The sediment source is in the shield, it consists mainly of crystalline rocks of the Guinea Highlands basement complex, together with Cretaceous and Tertiary sediment derived from the Cameroon volcanic zone. There are indicators that, the diapiric uplift of the delta front on the continental slope and rise is a major structural factor controlling progradation (Evamy et al., 1978; Whiteman, 1982).

Sedimentology and faunal data suggest that the modern Niger Delta has a configuration similar to the past (Benkheli et al., 1989). The present day Niger Delta is an overall regressive sequence of classic sediments developed in a series of offlap cycles (rift faulting) during the Precambrian (Weber, 1971). The base of the sequence consists of massive and monotonous marine shales, these grade upward into inter-bedded shallow-marine and fluvial sands, silts and clays which form the typical paralic facie portion of the delta. The uppermost of the sequence is a massive non-marine sand section. The total thickness of this composite sequence may reach 12km in the basin centre (Evamy et al., 1978). Gravity and magnetic data suggest that the maximum thickness lies in the area between Warri and Port Harcourt. While marine shales as old as Paleocene may underlie the entire complex with its deltaic facies ranging from Eocene in North to Miocene in the south.

The Niger Delta progradation has been controlled by synsedimentary fault,

folding and interplay between subsidence and sediment supply. The delta can be divided into a number of major growth-fault-bounded sedimentary units or "depobelts". Each depobelt contains one or more palaeontologically distinct transgressive interruptions in the overall regressive sequence that is probably related to the sea level rises. The result is a gradual increase in sand percentage up section. The interdigitation of lithofacies in the Niger Delta makes the stratigraphic nomenclature a difficult one, however, three formation names are in widespread use these include, the Benin Formation, Agbada Formation and Akata Formation (Short and Stauble, 1967; Weber, 1971; Evamy et al., 1978; Doust and Omatsola, 1990). This is the shallowest part of the sequence (Figure 2) which extends from the west across the whole Niger Delta area and southwards. It has over 90 percent of sandstone with shale intercalation. The formation was deposited in a continental fluvial environment and composed almost entirely of non-marine sand. It is coarse grained, poorly sorted and bears lignite streaks and wood fragments and partly unconsolidated. It has various structural unit such as point bars, channel fills, oxbow fills, all these indicate the variability of the shallow water depositional medium.

The oldest lacked fauna and is impossible to date correctly and may be Oligocene. It has various thickness that exceed 1820 metres and little hydrocarbon has been found in this formation (Short and Stauble, 1967; Kogbe, 1989). This formation overlies the Akata formation and it occurs in the subsurface of the whole Delta area (Figure 2). Its sequence is represented by an alternation of sands, silts and clays in various proportions. They are the truly deltaic portion of the sequence and are deposited in a number of delta-front, delta-topset and fluvio-deltaic environments. The sands are poorly sorted, round to sub-rounded, slightly consolidated but majority are unconsolidated. The sands grade it to the lower part of the formation, thus an alternation of fine and coarse clastic which provide multiple reservoir-seal couplets. More hydrocarbons have been found in the formation compared to the Benin formation.

Akata Formation (Figure 2) is the lowest unit and has a lithofacies composed of shales, clays and silts at base of the delta sequence. They contain a few streaks of sand, possible of turbidite origin and were deposited in holomarine (delta-front to deeper marine) environment. It is about 7000 metres thick at the central part of the delta. Thin sandstone lenses occur near the top particularly near the contact with the overlying Agbada formation. It crops out offshore in diaper along the continental slope and onshore in the north eastern part of the delta, where they are known as Imo Shales. Except on the basin flanks, no well has fully penetrated this sequence. The marine sequence is typically over pressure. It ranges in age from Paleocene to Holocene and this formation is thought of as the primary source rock for hydrocarbon over pressure. Problem arises with the definition of the top and base of the Agbada formation. The top is usually defined by local geologist as the base of freshwater invasion, whereas the base is often placed as the onset of hardover pressure during drilling. These problems arise because of local argillaceous intercalation in the lithofacies. Thus a detailed stratigraphy is complex. In view of this, it is recommended that this formation nomenclature only be used informally (Doust and Omatsola, 1990).

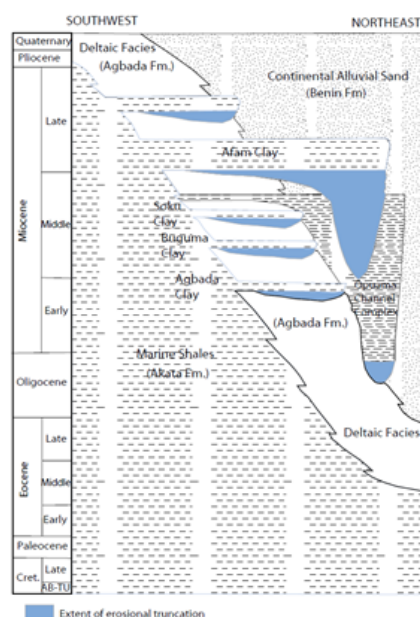


Figure 2: Stratigraphic column of the Niger Delta. Image from USGS Open-File Report 99-50-H (1999) and modified from Shannon and Naylor (1989) and Doust and Omatsola (1990).

3. THEORETICAL BACKGROUND

3.1 Interior Earth's Heatflow

The thermal state of the earth's interior is influenced by mass flow of magma in the mantle, which makes it highly unstable (Turcotte and Schubert, 1973; Andrew, 1975; Quike, 1980). The estimated total heat loss of the earth is 42×10^{12} watts (Sclater et al., 1980). Variation in heat flow are evident and this is due to temperature variation in a "convecting system" within the near-surface, such as region of volcanism in Rio Grade rift in the southern New Mexico (Decker and Smithson 1975; Erickson et al., 1975). Mechanism of heat transport includes conduction, convection and advection, out of which conduction is the most important. The basic equation for transport, is given by Fourier law, which is the heat flow per unit area (Q) at a point:

$$Q = -k \frac{dT}{dz} \quad (1)$$

where k = thermal conductivity; $\frac{dT}{dz}$ = geothermal gradient.

3.2 Mechanisms of Subsidence

All continental structures pass through a substantially different period of geologic history, with their diversity determined by diversified character of development. Subsidence as it were is evident in most if not all continental structures in various capacities and a geologic cross section of a typical major delta will show a depressed lithosphere on which there is an accumulation of several thousands of feet of sediments. This depression may be due to tectonic or simply as a result from the weight of sediment. In summary, since the sedimentary basin in Nigeria have their origin linked to extensional activities during the Mesozoic, models developed for the evolution and subsidence of continental margin and continental rift basin are similarity analysis, stretching model (Turcotte and Ahern, 1977; McKenzie, 1978). This involves phenomena of subsidence occurring in the oceanic ridge, at which it was created. This is also applicable to the continents which involves cooling of the lithosphere due to the sediment loading or/and heat from the mantle. Total subsidence is as a result of tectonic subsidence, load induced subsidence, water depth, sea level changes, compaction. There may be two types of possible mechanisms of subsidence, namely (Middleton, 1982):

3.3 Thermal Contraction of Lithosphere

Cooling of a lithospheric plate, particularly young oceanic crust or recently stretched continental crust, causes thermal subsidence. As the plate cools it shrinks and becomes denser through thermal contraction. Analogous to a solid floating in a liquid, as the lithospheric plate gets denser it sinks because it displaces more of the underlying mantle through an equilibrium process known as isostasy. Thermal subsidence is particularly measurable and observable with oceanic crust, as there is a well-established correlation between the age of the underlying crust and depth of the ocean. As newly-formed oceanic crust cools over a period of tens of millions of years. This is an important contribution to subsidence in rift basins, backarc basins and passive margins where they are underlain by newly-formed oceanic crust. Rift basins are elongate sedimentary basins formed in depressions created by tectonically-induced thinning (stretching) of continental crust, generally bounded by normal faults that create grabens and half-grabens, Figure 3 (Burke, 1985).

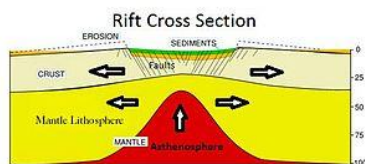


Figure 3: Typical rift formation in cross-section (https://en.wikipedia.org/wiki/Sedimentary_basin#/media/File:Riftxsection.jpg, 2023)

3.4 Phase Change Mechanism

Middleton proposed a model of phase change (metamorphism) in the deep crust based on a one-dimensional "solidification" boundary entailing a change of volume with phase change (Middleton, 1982). This change occurs in response to heating from a maintained magma chamber below the Moho. The displacement of the phase boundary, Z, is related to the magnitude of basement subsidence, S, by the equation:

$$S = \frac{D_m(D_2 - D_1)Z}{D_1(D_m - D_s)} \quad (2)$$

where D_m = Density of mantle; D_s = Density of sediment; D_1 = Density of magnesian; D_2 = Density of ultra-basic rock. The type of basin formed is the strike-slip basin, Figure 4, where D_m = Density of mantle; D_s = Density of sediment; D_1 = Density of magnesian schist; D_2 = Density of ultrabasic rock.

4. MATERIALS AND METHODS

Four wells Well-1, Well-2, Well-3 and Well-4, were used in this study. The study started with the preliminary collection of oil well data such as Gamma, Sonic and Formation density logs together with their bio-stratigraphic data and prospect area maps from petroleum exploratory wells provided by Shell Petroleum Development Company (East) and Elf Petroleum Nigeria Limited. The interval interpreted in these wells falls in the Benin and Agbada Formations of the Niger Delta basin. Each ranges in depth from the surface to over 3700m. The wells either had the bore hole compensated Sonic, Gamma or Compensated formation density.

4.1 Determination of Sand/Shale Volume

This was carried out by first delineating sections of each Gamma log run for the different wells at an interval of 500 feet into three lithofacies use, either sandstone or shale or shaly-sand based on their shaliness and API unit values. For sandstone API unit used ranges between zero (0) and about 30 API units. For shaly-sand 30-80 API units was used. While for shale, API units value greater than 80 was assigned. The amount of each lithofacies is then estimated by counting the interval of a particular lithofacies has occurred and then assigns a fraction of this to the total interval which is then expressed as a percentage.

4.2 Determination of Porosity

The porosity of the lithologies in the various wells was estimated using Sonic log and equation (Wylie's et al., 1958):

$$\phi_s = \frac{\Delta t_{\log} - \Delta t_{ma}}{\Delta t_f - \Delta t_{ma}} \quad (3)$$

where Δt_{\log} = transient time from sonic log; Δt_{max} = transient time of matrix; Δt_f = transient time of fluid. The constants for various material matrix density and matrix transit time are given in Tables 1.

4.3 Determination of Thermal Conductivity

Thermal conductivity depends on the conductivity of each constituent of the rock, its porosity and the saturating fluid conductivity, this is expressed as (Kaichi, 1984):

$$K_s = K_f^\phi k^{1-\phi} \quad (4)$$

where K_s = Conductivity of rock; K_m = Conductivity of matrix; K_f = Conductivity of fluid; ϕ = Porosity.

But when there is more than one matrix in a particular layer, for example sand, then

$$K_m = K_1^{\lambda_1} K_2^{\lambda_2} K_3^{\lambda_3} \dots K_n^{\lambda_n} \quad (5)$$

where $K_1 \dots K_n$ = various matrix conductivity; $\lambda_1 \dots \lambda_n$ = fractional percentages.

4.4 Determination of Geothermal Gradient (G)

Geothermal gradient can be computed by using Thermal resistance method otherwise known as Bullard method (Chapman et al., 1985). This is used to judge the ability of petroleum well bottom-hole temperature data in determining surface heat flow and sub-surface temperature patterns in a sedimentary basin. The second method was used in this study based on the relevant availability of data supplied. Average surface temperature was to be 27°C. While the bottom whole temperature (BHT) for various well gotten from the log and their corresponding depth.

$$G = \frac{dT}{dz} = \frac{T_o C - T_o C}{\partial_m - \partial_o} \quad (6)$$

where T^o = Bottom hole temperature; T^s = Surface temperature; δ_m = Total depth drilled (m); δ_o = Ground surface (m). The BHTs for Wells 1, 2, 3 and 4 were 72.22°C, 78.33°C, 110.0°C, and 93.33°C respectively.

Rocks	Thermal Conductivity (Wm ⁻¹ K ⁻¹)
Shale	2.7
Sandstone	7.0
Silt	6.0
Water	0.6

4.5 Determination of Heat Flow

With the assumption that the main mechanism of heat flow is by conduction in sedimentary Niger Delta basin, the Fourier law for heat flow transport applies and is given as,

$$Q = K_s \frac{dT}{dz} \tag{7}$$

where Q = Heat flow (Wm⁻²); K_s = Conductivity (Wm⁻¹K⁻¹); $\frac{dT}{dz}$ = Geothermal gradient (°Cm⁻¹).

4.6 Determination of Burial History and Total Subsidence

Rate of subsidence (Turcotte and Ahern, 1977), V:

$$V = A_0 t^{-1/2} \tag{8}$$

where $A_0 = \frac{\rho_m \alpha_m (T_m - T_0)}{\rho_m - \rho_s} \left(\frac{k_m}{\pi} \right)^{1/2}$ is a function of hot mantle rock under the basin.

where $\rho_m = 3330\text{kgm}^{-3}$ (Mantle density); $\alpha_m = 3 \times 10^{-5}\text{C}^{-1}$ - Coefficient of thermal expansion of Mantle; $T_m = 1350^\circ\text{C}$ (Temperature of Mantle); $T_0 = 27^\circ\text{C}$ (Initial background temperature); $K_m = 3.1\text{Wm}^{-1}\text{K}^{-1}$ (Thermal conductivity of Mantle); $\pi = 3.142$; ρ_s = average sediment density; is 2180.0kgm⁻³ for well-1; is 2098.0kgm⁻³ for well-2; is 2285.6kgm⁻³ for well-

3, and is 2253.1kgm⁻³ for well-4. The burial history, the depth of a sedimentary basin with age t-t_s has age t in the sedimentary basin:

$$Y_s = 2A_0 \left(t^{1/2} - t_s^{1/2} \right) \tag{9}$$

where t = geologic time; t_s = time after subsidence initiation, taken as 0, 5, 10, 15,...these values are plotted against age.

Depth of sedimentary basin,

$$Y_{sb} = 2A_0 t^{-1/2} \tag{10}$$

4.7 Determination of Tectonic Subsidence (Y)

$$Y = S \bullet B_0 + W_d - \Delta SL \tag{11}$$

where $B_0 = \frac{\rho_m - \rho_s}{\rho_m}$; Y = tectonic subsidence; W_d = water depth; S = sediment thickness; ΔSL = changes in sea level; B₀ is a value related to the hot mantle rock under the basin with the assumption that W_d = 0 = ΔSL , this is as a result of some findings that, there is no significant difference from present in the sea level of post Cretaceous subsidence and deposition of the Niger Delta sediment (Sclater et al., 1980; Onuoha and Ofoegbu, 1987).

5. RESULTS AND DISCUSSION

5.1 Stratigraphic Units

The interpretation of delineation of wells into strata was based upon three lithofacies, namely, sandstone, shaly sand and shale. This was based on the Gamma ray log used for the four wells, and their sand-shale percentage estimated (Table 4). There was the general trend of the massive sandstones in the upper layers, characteristics of the Benin formation into an alternation of both sandstone and shales characteristic of the Agbada formation, followed by an increase in shale percentage down the series. However, the four wells did not bottom the Akata formation as the total depth drilled are in the range of 2865.1m - 3718.6m. The bottom of the Benin/top of Agbada boundaries for the four wells are about 1524.0m, 1066.8m, 1981.2m and 1371.6m for Wells 1, 2, 3 and 4 respectively.

Depth (ft)	Depth (m)	Sand %	Shale %	Δt (μ sec/ft)	Porosity φ (%)	Thermal conductivity, k _s (Wm ⁻¹ K ⁻¹)
0-500	0-152.4	100	0	113.85	43.38	2.411
500-1000	152.4-304.8	100	0	113.85	43.38	2.411
1000-1500	304.8-457.2	100	0	113.85	43.38	2.411
1500-2000	457.2-609.6	100	0	113.85	43.38	2.411
2000-2500	609.6-762.0	94	6	113.85	43.38	2.411
2500-3000	762.0-914.4	100	0	113.85	43.38	2.411
3000-3500	914.4-1066.8	100	0	113.85	43.38	2.411
3500-4000	1066.8-1219.2	100	0	113.85	43.38	2.411
4000-4500	1219.2-1371.6	96	4	125.94	52.4	1.892
4500-5000	1371.6-1524.0	96	4	119.90	47.9	2.109
5000-5500	1524.0-1676.4	82	18	114.90	44.2	2.148
5500-6000	1676.4-1828.8	88	12	113.82	43.4	2.250
6000-6500	1828.8-1981.2	86	14	111.86	41.9	2.307
6500-7000	1981.2-2133.6	96	4	101.86	34.5	2.913
7000-7500	2133.6-2286.0	64	36	96.86	30.8	2.601
7500-8000	2286.0-2438.4	46	54	91.86	27.0	2.483
8000-8500	2438.4-2590.8	64	36	87.84	24.0	3.007
8500-9000	2590.8-2743.2	50	50	80.85	18.9	3.019
9000-9500	2743.2-2895.6	8	92	81.86	43.1	1.470
9500-10000	2895.6-3048.0	64	36	79.80	18.1	3.407
10000-10500	3048.0-3200.4	0	100	78.82	41.5	1.447
10500-11000	3200.4-3352.8	66	34	74.90	14.4	3.748
11000-11500	3352.8-3505.2	0	100	79.90	41.6	1.445
11500-11900	3505.2-3627.1	75	25	79.90	18.1	3.685

Table 4b: Sand-Shale Percentage, Porosity and Thermal Conductivity for Well-2

Depth (ft)	Depth (m)	Sand (%)	Shale (%)	Δt ($\mu\text{sec}/\text{ft}$)	Porosity, ϕ (%)	Thermal Conductivity k_s ($\text{Wm}^{-1}\text{K}^{-1}$)
0-500	0-152.4	100	0	113.85	43.38	2.411
500-1000	152.4-304.8	100	0	113.85	43.38	2.411
1000-1500	304.8-457.2	94	6	113.85	43.38	2.335
1500-2000	457.2-609.6	98	2	113.85	43.38	2.386
2000-2500	609.6-762.0	94	6	113.85	43.38	2.335
2500-3000	762.0-914.4	94	6	113.85	43.38	2.335
3000-3500	914.4-1066.8	92	8	121.86	49.3	2.007
3500-4000	1066.8-1219.2	72	28	116.78	45.6	1.982
4000-4500	1219.2-1371.6	40	60	108.78	39.6	1.887
4500-5000	1371.6-1524.0	76	24	104.80	36.6	2.474
5000-5500	1524.0-1676.4	54	46	96.77	30.7	2.422
5500-6000	1676.4-1828.8	38	62	91.77	27.0	2.353
6000-6500	1828.8-1981.2	76	24	89.90	25.6	3.160
6500-7000	1981.2-2133.6	44	56	87.84	24.1	2.580
7000-7500	2133.6-2286.0	40	60	90.92	26.3	2.428
7500-8000	2286.0-2438.4	8	92	93.82	49.4	1.335
8000-8500	2438.4-2590.8	78	22	83.86	21.1	3.545
8500-9000	2590.8-2743.2	0	100	84.90	44.7	1.379
9000-9400	2743.2-2865.1	0	100	96.86	51.0	1.254

Table 4c: Sand-Shale Percentage, Porosity and Thermal Conductivity for Well-3

Depth (ft)	Depth (m)	Sand (%)	Shale %	Bulk density, ρ_b (g/cm^3)	Porosity ϕ (%)	Thermal Conductivity k_s ($\text{Wm}^{-1}\text{K}^{-1}$)
0-4000	0 - 1219.2	100	0	1.97	43.38	2.411
4000-4500	1219.2-1371.6	100	0	1.97	43.38	2.411
4500-5000	1371.6-1524.0	94	6	1.97	43.38	2.335
5000-55000	1524.0-1676.4	98	2	1.97	43.38	2.386
5500-6000	1679.4-1828.8	94	6	1.97	43.38	2.335
6000-6500	1828.8-1981.2	84	16	2.00	41.6	2.303
6500-7000	1981.2-2133.6	40	60	2.18	30.1	2.261
7000-7500	2133.6-2286.0	8	92	2.24	37.1	1.616
7500-8000	2286.0-2438.4	4	96	2.56	19.6	2.071
8000-8500	2438.4-2590.8	20	80	2.47	24.5	2.172
8500-9000	2590.8-2743.2	18	82	2.27	35.4	1.770
9000-9500	2743.2-2895.6	2	98	2.39	28.9	1.794
9500-10000	2895.6-3048.0	12	88	2.29	34.9	1.712
10000-10500	3048.0-3200.4	6	94	2.87	3.0	2.762
10500-11000	3200.4-3352.8	0	100	2.87	3.0	2.582
11000-11500	3352.8-3505.2	4	96	2.87	3.0	2.582
11500-12000	3305.2-3657.6	0	100	2.87	3.0	2.582
12000-12200	3657.6-3718.6	0	100	2.87	3.0	2.582

Table 4d: Sand-Shale Percentage, Porosity and Thermal Conductivity for Well-4

Depth (ft)	Depth (m)	Sand %	Shale %	Bulk density ρ_b (g/cm^3)	Porosity ϕ (%)	Thermal Conductivity k_s ($\text{Wm}^{-1}\text{K}^{-1}$)
0-500	0-152.4	100	0	1.97	43.38	2.411
500-1000	152.4-304.8	100	0	1.97	43.38	2.411
1000-1500	304.8-457.2	90	10	1.97	43.38	2.172
1500-2000	457.2-609.6	100	0	1.97	43.38	2.411
2000-2500	609.6-762.0	96	4	1.97	43.38	2.360
2500-3000	762.0-914.4	98	2	1.97	43.38	2.386
3000-3500	914.4-1066.8	100	0	1.97	43.38	2.411
3500-4000	1066.8-1219.2	78	22	1.97	43.38	2.138
4000-4500	1219.2-1371.6	90	10	2.30	22.4	3.767
4500-5000	1371.6-1524.0	84	16	2.32	21.1	3.692
5000-5500	1524.0-1676.4	68	32	2.15	32.0	2.605
5500-6000	1676.4-1828.8	86	14	2.17	30.7	2.993
6000-6500	1828.8-1981.2	94	6	2.17	30.7	2.960
6500-7000	1981.2-2133.6	18	82	2.35	19.2	2.322
7000-7500	2133.6-2286.0	40	60	2.21	28.1	2.347
7500-8000	2286.0-2438.4	0	100	2.15	42.0	1.436
8000-8500	2438.4-2590.8	16	84	2.18	40.4	1.598
8500-9000	2590.8-2743.2	0	100	2.26	36.0	1.571
9000-9500	2743.2-2895.6	0	100	2.27	35.4	1.587
9500-10000	2895.6-3048.0	0	100	2.28	34.9	1.598
10000-10500	3048.0-3200.4	10	90	2.34	31.6	1.804
10500-11000	3200.4-3352.8	0	100	2.41	27.8	1.779
11000-11500	3352.8-3505.2	0	100	2.37	30.0	1.719
11500-11700	3505.2-3566.2	15	85	2.41	27.8	1.964

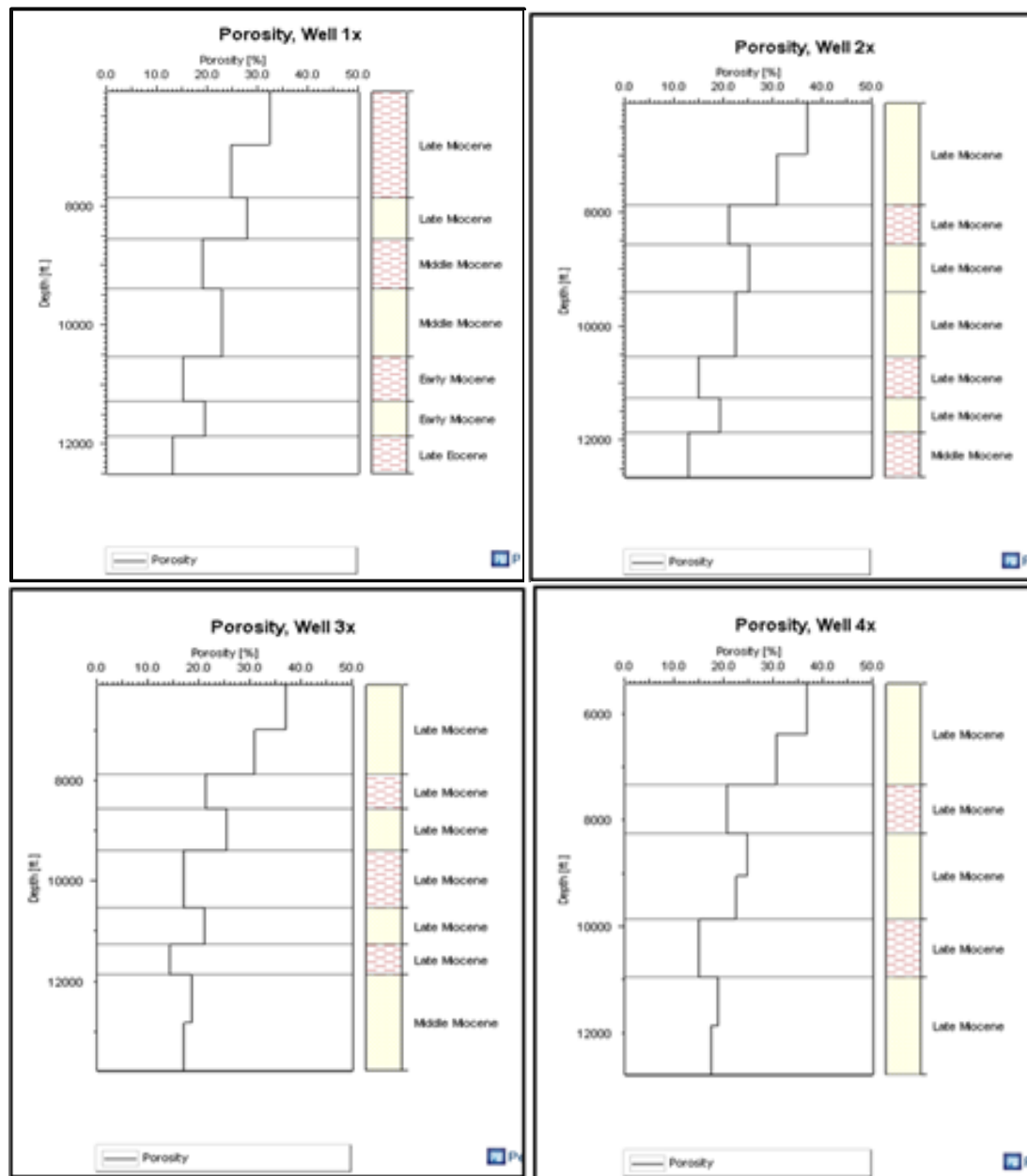


Figure 5: Porosity-Depth profiles for the Wells

The Benin formation exhibit higher thermal conductivity, this is due to the high percentage of sandstone in the formation which has a high thermal matrix conductivity of $7\text{Wm}^{-1}\text{K}^{-1}$ (Table 3). The porosity itself decreases with increase in depth. A plot of porosity-depth is shown for the four wells (Figures 5).

5.2 Porosity and Thermal Conductivity

The porosity (Figure 5) and thermal conductivity (Table 4) varies with lithology and depth. The average thermal conductivity for Benin formation for the wells are about $2.36\text{Wm}^{-1}\text{K}^{-1}$, $2.27\text{Wm}^{-1}\text{K}^{-1}$, $2.35\text{Wm}^{-1}\text{K}^{-1}$, and $2.55\text{Wm}^{-1}\text{K}^{-1}$ for Wells 1, 2, 3 and 4 respectively. Porosity determines the volume of hydrocarbons a reservoir may hold, as such, it is a critical attribute in reservoir analysis. Results obtained from thermal conductivity models showed highly variable values with depth. The thermal conductivity values fell within the range obtainable in the Niger Delta from the works of (Akpabio, 2009; Emujakporue, 2009; Odumodu, 2011).

5.3 Geothermal Gradient and Heat Flow

The geothermal gradient for the four wells are $1.247^\circ\text{C}/100\text{m}$, $1.792^\circ\text{C}/100\text{m}$, $2.232^\circ\text{C}/100\text{m}$ and $1.862^\circ\text{C}/100\text{m}$. The variations in the geothermal gradients in the Niger Delta can be attributed to the lithological changes or sedimentation rate in the area. Regions with low geothermal gradients are known to correspond with areas of high percentage of sands because sands are better conductors than shale, on the other hand higher geothermal gradients are attributed to high shale volume, as such, in the Niger Delta minimal thermal gradients usually tend

to coincide with areas of maximum thickness of the sandy Agbada and Benin Formation, while maximum thermal gradients occurs at delta fronts where the deeper Akata Formation exerts a stronger influence. Geothermal Gradients variations play a significant role in source rock maturation. Heat flow values are 30.73mWm^{-2} , 40.57mWm^{-2} , 50.53mWm^{-2} and 40.19mWm^{-2} . This trend follows higher bottom hole temperature, thus high geothermal gradient which then brings about higher heat flow (Table 5). The result agrees with the concept of temperature influence on heat flux (Sass et al., 1976).

5.4 Burial History and Subsidence Rate

Subsidence history analysis, adopting Niger Delta Chronological Chart, on wells showed that there was similar trend across all fields modelled (Nwaamaka et al., 2015). Firstly, a rapid phase of subsidence which started in the early to Middle Miocene between 6.5Ma to 10Ma, this phase of subsidence created accommodation for sediments of an average thickness of 5,000ft to be deposited, this was followed by a period of gradual uplift which lasted between 3.5Ma in the Mid-Pliocene to 6.5Ma in the Early Miocene, when there was erosion of surface sediments across the basin. A more progressively rapid subsidence episode took place between the Middle Pliocene at 3.5Ma which lasted till the Early-Pleistocene creating accommodation for the deposition of sediments with an average thickness of 1066.57m. Sediments loading contributes in major way to the observed subsidence, however, there still a large residual subsidence due to other causes such as the tectonic driving forces, otherwise known as Tectonic subsidence.

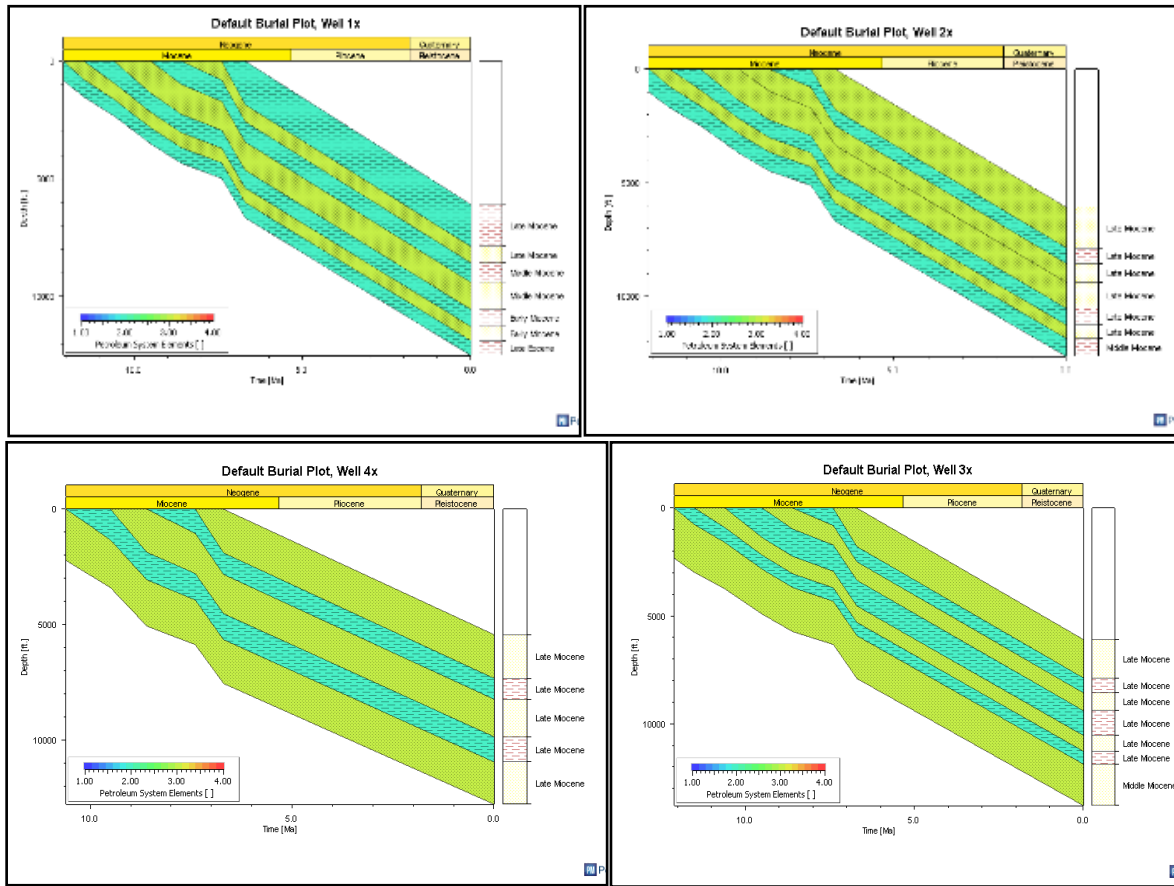


Figure 6: Burial Curves of the Wells

Table 5: Temperature, Geothermal Gradient and Heat Flow for Wells			
Well	Bottom Hole Temperature (°C)	Geothermal gradient, G, (°C/100m)	Heat flow value, Q, (mWm ⁻²)
1	72.22	1.247	30.73
2	78.33	1.792	40.57
3	110.0	2.232	50.57
4	93.33	1.860	42.19
Average	88.47	1.78275	41.015

Table 6a: Biostratigraphic Data, Rate of Subsidence and Depth to Sedimentary Basin For Well-1								
Depth (ft)	Depth (m)	Age (Ma)	Porosity, φ (%)	Sand %	Shale %	Density (kgm ⁻³)	V (mMa ⁻¹)	Y _{sb} (m)
0-5119	0-1560.3	19.5	44.2	82	18	1959.0	0.0147	572.8
5119-6761	1560.3-2060.8	20.8	34.5	96	4	2110.0	0.0142	591.6
6761-701	2060.8-2149.2	23.3	30.8	64	36	2168.0	0.0134	626.1
7051-728	2149.2-2215.3	21.6	30.8	64	36	2168.0	0.0140	602.8
7268-7945	2215.3-2421.6	21.6	27.0	46	54	2228.0	0.0140	602.8
7945-7995	2421.6-2436.9	25.9	24.0	64	36	2275.0	0.0127	660.1
7995-9369	2436.9-2855.7	30.7	43.1	8	92	2130.0	0.0117	718.6
9369-11062	2855.7-3371.7	29.9	14.4	66	34	2425.0	0.0119	709.3
11062-11400	3371.7-3474.7	30.7	41.6	0	100	2157.0	0.0117	718.6
Average							0.013144	644.744

Table 6b: Biostratigraphic Data, Rate of Subsidence and Depth to Sedimentary Basin For Well-2:								
Depth (ft)	Depth (m)	Age (Ma)	Porosity, φ (%)	Sand %	Shale %	Density (kgm ⁻³)	V (mMa ⁻¹)	Y _{sb} (m)
0-1408	0-429.2	17.3	43.38	94	6	1972.0	0.0256	886.4
1408-1775	429.2-541.0	19.3	43.38	98	2	1972.0	0.0243	936.3
1775-2310	541.0-704.1	23.3	43.38	94	6	1972.0	0.0221	1028.7
2310-3171	704.1-966.5	25.9	49.3	92	8	1879.0	0.0209	1084.6
3171-3691	966.5-1125.0	29.5	45.6	72	28	1936.8	0.0196	1157.5
3691-4456	1125.0-1358.2	31.7	39.6	40	60	2030.7	0.0189	1199.9
4456-5060	1358.2-1542.3	34.2	36.6	76	24	2077.6	0.0182	1246.3
5060-5192	1542.3-1582.5	34.3	30.7	54	46	2169.8	0.0182	1248.2
5192-5609	1582.5-1709.6	34.2	27.0	38	62	2424.8	0.0182	1246.3
5609-6324	1709.6-1927.6	36.0	25.6	76	24	2249.6	0.0178	1278.7
6324-6751	1927.6-2057.7	35.5	24.1	44	56	2478.0	0.0179	1269.8
6751-8041	2057.7-2450.9	35.5	49.4	8	92	2014.0	0.0179	1269.8
Average							0.019967	1154.375

Table 6c: Biostratigraphic Data, Rate of Subsidence and Depth to Sedimentary Basin for Well-3:

Depth (ft)	Depth (m)	Age (Ma)	Porosity, ϕ (%)	Sand %	Shale %	Density (kgm^{-3})	V (mMa^{-1})	Y_{sb} (m)
0-800	0-243.8	3.0	43.38	100	0	1972.0	0.0725	435.5
800-1200	243.8-365.8	4.0	43.38	100	0	1972.0	0.06229	502.8
1200-2300	365.8-701.0	5.0	43.38	100	0	1972.0	0.0562	562.2
2300-2880	701.0-877.8	6.0	43.38	100	0	1972.0	0.0513	616.0
2880-3520	877.8-1072.9	9.0	43.38	100	0	1972.0	0.0419	754.3
3520-4500	1072.9-1321.6	14.0	43.38	100	0	1972.0	0.0336	940.8
4500-5840	1321.6-1780.0	18.0	43.38	100	0	1972.0	0.0296	1066.8
5840-6400	1780.0-1950.7	20.0	41.6	84	16	2180.0	0.0281	1124.8
6400-7600	1950.7-2316.5	21.0	5.8	4	96	2560.0	0.0274	1152.2
7600-8050	2316.5-2453.6	22.0	11.5	20	80	2470.0	0.0268	1179.2
8050-9480	2453.6-2889.5	23.0	16.6	0	100	2390.0	0.0262	1205.8
9480-10600	2889.5-3230.9	26.0	3.0	0	100	2865.0	0.0247	1282.0
10600-11200	3230.9-3413.8	29.0	3.0	0	100	2865.0	0.0233	1353.9
11200-12200	3413.8-3718.6	30.0	3.0	0	100	2865.0	0.0229	1377.0
Average							0.037628	968.0929

Table 6d: Biostratigraphic Data, Rate of Subsidence and Depth to Sedimentary Basin for Well-4

Depth (ft)	Depth (m)	Age (Ma)	Porosity ϕ (%)	Sand %	Shale %	Density (kgm^{-3})	V (mMa^{-1})	Y_{sb} (m)
0-3850	0-1178.5	9.0	43.38	78	22	1972.0	0.0406	731.4
3850-4990	1178.5-1521.0	14.0	21.1	84	16	2320.0	0.0326	912.3
4990-6520	1521.0-1987.3	18.0	19.2	18	82	2350.0	0.0287	1034.4
6520-7130	1987.3-2173.2	20.0	28.1	40	60	2210.0	0.02273	1090.4
7130-9480	2173.2-2889.5	21.0	35.4	0	100	2270.0	0.0266	1117.3
9480-9940	2889.5-30291.7	22.0	34.9	0	100	2280.0	0.0260	1143.6
9940-11530	3029.7-3514.3	23.0	30.0	0	100	2370.0	0.0254	1169.3
Average							0.028947	1028.386

Table 7a: Computed Values for Burial History for Well-1

Time (x 10 ⁶ Yrs)	ts = 0 (m)	ts = 5 (m)	ts = 10 (m)	ts = 15 (m)	ts = 20 (m)	ts = 25 (m)	ts = 30 (m)
19.5	572.76	282.75	161.64	70.43			
20.8	591.56	301.55	181.45	89.23	11.54		
21.6	602.85	312.84	192.73	100.52	22.83		
23.3	626.06	336.05	215.95	123.73	46.04		
25.9	660.04	370.03	249.93	157.72	80.03	11.54	
29.9	709.20	419.19	299.09	206.87	129.19	60.7	
30.7	718.67	428.66	308.56	216.34	138.65	70.17	8.30

Table 7b: Computed Values for Burial History for Well-2

Time (x 10 ⁶ Yrs)	ts = 0 (m)	ts = 5 (m)	ts = 10 (m)	ts = 15 (m)	ts = 20 (m)	ts = 25 (m)	ts = 30 (m)	ts = 35 (m)
17.3	886.36	409.83	212.48	60.95				
19.3	936.23	459.70	262.35	110.82				
23.3	1028.73	552.19	354.84	203.32	75.66			
25.9	1084.56	608.03	410.69	259.15	131.50	18.97		
29.5	1157.45	680.92	483.57	332.04	204.38	91.85		
31.7	1199.86	723.33	525.98	374.45	246.79	134.27	32.61	
34.2	1246.32	769.79	572.44	420.91	293.25	180.73	79.07	
34.3	1248.24	771.70	574.36	422.83	295.17	182.64	80.99	
35.5	1269.76	793.23	595.88	444.35	316.70	204.17	102.51	8.95
36.0	1278.72	802.18	604.83	453.30	325.65	213.12	111.46	17.90

Table 7c: Computed Values for Burial History for Well-3

Time (x 10 ⁶ Yrs)	ts = 0 (m)	ts = 5 (m)	ts = 10 (m)	ts = 15 (m)	ts = 20 (m)	ts = 25 (m)	ts = 30 (m)
3.0	435.50						
4.0	502.83	0					
6.0	615.97	53.80					
9.0	754.25	192.08					
14.0	940.80	378.68	145.80				
18.0	1066.76	504.59	271.78	93.02			
20.0	1124.34	562.17	329.36	150.60	0		
21.0	1150.24	590.07	357.26	178.51	27.91		
22.0	1179.15	616.98	384.17	205.14	54.81		
23.0	1205.80	643.68	410.82	232.06	81.46		
26.0	1281.20	719.81	486.99	308.24	157.64	24.89	
29.0	1353.88	791.71	558.90	380.14	229.54	96.80	
30.0	1377.01	814.84	582.03	423.27	252.67	119.93	0

Table 7d: Computed Values for Burial History for Well-4

Time (x 10 ⁶ Yrs)	ts = 0 (m)	ts = 5 (m)	ts = 10 (m)	ts = 15 (m)	ts = 20 (m)
9.0	731.44	186.27			
14.0	912.35	367.18	141.41		
18.0	1034.50	489.33	263.56	90.21	
20.0	1090.33	545.17	319.40	146.04	0
21.0	1117.40	572.23	346.46	173.11	27.06
22.0	1143.49	598.32	372.55	199.20	53.15
23.0	1169.33	624.16	398.39	225.04	79.00

Table 8a: Computed Value for Tectonic Subsidence for Well-1

Time (x 10 ⁶ yr)	Depth (m)	S* (m)	Y (m)
0-22	35	35	12.09
22-27	105	70	24.17
27-32	180	75	25.90
32-38	275	95	32.81
38-42	385	110	37.95
42-46	580	195	67.34
46-51	830	250	86.34

Table 8b: Computed Value for Tectonic Subsidence for Well-2

Time (x 10 ⁶ yr)	Depth (m)	S* (m)	Y (m)
0-17	87.5	87.5	32.37
17-22	200.0	112.5	41.62
22-27	325.0	125.0	46.25
27-32	462.5	137.5	50.87
32-37	612.50	150.0	55.49
37-41	787.50	175.0	64.75
41-46	975.0	187.5	69.37
46-51	1500.0	525.0	194.23

Table 8c: Computed Value for Tectonic Subsidence for Well-3

Time (x 10 ⁶ yr)	Depth (m)	S* (m)	Y (m)
0-27	150	150	47.05
27-32	300	150	47.05
32-37	460	160	50.18
37-42	640	180	56.45
42-47	890	250	78.41
47-52	1200	310	97.23

Table 8d: Computed Value for Tectonic Subsidence for Well-4

Time (x 10 ⁶ yr)	Depth (m)	S* (m)	Y (m)
0-4	80	80	25.87
4-8	240	160	51.74
8-11	400	240	77.61
11-18	650	250	80.85
18-23	1120	470	152.00

6. DISCUSSION

6.1 Implication of Geothermal Gradient

The thermal gradient determined for intervals of Benin and Agbada formations varied as a result of thermal conductivity of the sediment variation in each of these interval. This in essence affected the heat flux too and possible reason for such variation could be linked to over pressure or/ and under pressure within the sediment as a result of radioactivity or sedimentation rate, or possibly the underlying crust, or still hydrothermal effects. In this study, the variation is linked to overpressure as observed in their porosity values, especially in the Agbada formation layer. The porosity rather than decreasing may be high for a particular layer.

Over pressure may have occurred as a result of tectonic activity, that is, if at a particular substratum layer, the pressure was normal, it can increase as a result of tectonic activity such as doming of Akata shale into the Agbada formation (Evamy et al., 1978). Tectonic activity in the Niger Delta has been reported by (Short and Stauble, 1967; Weber, 1971; Evamy et al., 1976; Kogbe, 1989). Over pressure may also occur when marsh localised gas is encountered as a result of exothermic chemical reaction such as gypsum forms, from anhydrites or when "hot" shale is encountered, this may be the result in Well-3 that has abnormal porosity (Table 4) variation. Though shale is porous sometimes and uncompacted shale may have as

high as 50% - 60% porosity, but for all practical purposes, it is assumed to be impermeable. However, this result in Well-3 or/and in the other wells is not confirmed as there were no core samples to carry out the necessary analysis. While under pressure is due mainly to tectonic activity.

The south Atlantic proceeded the breaking up of the south America from Africa and as a result, new crust is being formed, the heat generated for its formation may have affected the estimated heat flux (Machens, 1973). There is adequate groundwater distribution in Nigeria, especially in the Southern part which serve as a means of heat transfer, convective mechanism, such that heat can be transferred from the inner crust up to the near subsurface (Oguntoyindo et al., 1978). However, the maximum heat flux estimated in this study 50.57mWm⁻² almost agrees with that estimated for a crust of this age, 100 million years, which is 54.46mWm⁻² while the heat flow value of a continental margin basin at the end of its rifting 62mWm⁻² (Sclater et al., 1980).

Uko obtained isoflux variation of 39.70mWm⁻² to a maximum value of 64.28mWm⁻² in the northern Niger Delta where this study was carried out, this is in agreement with the estimated heat flux gotten in this study approximately, while presented heat flux variation in the entire Niger Delta of the marine-paralic section to be 20mWm⁻² to 61mWm⁻² this is also in agreement with the result of this study (Uko, 1996; Akpabio, 1997). Onuoha predicted near-surface geothermal of 3.65°C/100m with a

thermal conductivity of $1.7\text{Wm}^{-1}\text{K}^{-1}$ has been reasonable (Onuoha, 1985). A group of researchers obtained geothermal gradient range of $1.73^\circ\text{C}/100\text{m}$ to $2.31^\circ\text{C}/100\text{m}$ with average of $2.100^\circ\text{C}/100\text{m}$ in eastern Niger using BHT data (Uko et al., 2021). Although actual values will depend on the dominant lithologies and local anomalies which may be the reason for the variation (Erickson et al., 1975).

6.2 Implication of Burial History and Subsidence Rate

The results (Table 6; Figure 6) show a subsidence rate of 0.013144mMa^{-1} to 0.037628mMa^{-1} , with a simple of 0.02538mMa^{-1} for all the four wells, subsidence seems to have started in the Oligocene and/or post Oligocene. This period corresponds to the period of rapid regression when the delta complex spread onto the cooling oceanic crust and buried much of the triple junction so increasing sediment load on an already cooling and foundering oceanic basement (Whiteman, 1982). Generally, subsidence curves show an initial rate which may have corresponded to the period of renewed subsidence after the complete separation of the continent of the early drift phase in the evolution of the Niger Delta, this is then followed by an increasing rate which correspond to the rapid regression stage and the burying of the triple junction, this is then followed by a normal decay rate. Analysis based on the rate of subsidence and sediment accumulation and compaction may permit sensitive detection of earlier stages in the evolution of compressional stress system and tectonic events. Also the thermal history and subsidence history may provide a clue to the palaeotemperature which then provide the basis for the degree of maturation of organic matter within the sediment.

6.3 Implication of Hydrocarbon Occurrence

Organic matter in sedimentary rocks generates petroleum under favourable temperature conditions. Temperature therefore plays the most important role in maturation of source rocks and oil and gas generation. Temperature usually increases with depth and the rate of increase with depth (geothermal gradient) is a prerequisite in the source rock potential evaluation. The geothermal gradients in wells -1, -2, -3 and -4 are $1.247^\circ\text{C}/100\text{m}$, $1.792^\circ\text{C}/100\text{m}$, $2.232^\circ\text{C}/100\text{m}$ and $1.862^\circ\text{C}/100\text{m}$ respectively. The average geothermal gradient $1.767^\circ\text{C}/100\text{m}$ for the field of study. The temperature of the source rocks in wells -1, -2, -3, and -4 are 72.22°C , 78.33°C , 110.0°C , and 93.33°C respectively. Since oil generation begins from 50°C , or from 60°C , the above temperature values show that oil generation is possible from the shale beds of Agbada Formation in the field of study (Hyne, 1984; Selley, 1996; Eliseus et al., 2012). This implies that these shales are thermally matured, and can generate crude oil if they contain enough kerogen.

7. CONCLUSION

The geothermal gradients in wells -1, -2, -3 and -4 are $1.247^\circ\text{C}/100\text{m}$, $1.792^\circ\text{C}/100\text{m}$, $2.232^\circ\text{C}/100\text{m}$ and $1.862^\circ\text{C}/100\text{m}$ respectively, based on an average surface temperature of 27°C . The average geothermal gradient $1.767^\circ\text{C}/100\text{m}$ for the field of study. Thermal conductivity values were highly variable with depth with values of $2.36\text{Wm}^{-1}\text{K}^{-1}$, $2.27\text{Wm}^{-1}\text{K}^{-1}$, $2.35\text{Wm}^{-1}\text{K}^{-1}$, and $2.55\text{Wm}^{-1}\text{K}^{-1}$ for Wells 1, 2, 3 and 4 respectively. The porosity and thermal conductivity varies with lithology and depth. The heat flux obtained for the wells are accordingly 30.73mWm^{-2} , 40.57mWm^{-2} , 50.53mWm^{-2} , and 42.19mWm^{-2} . There was the general trend of the massive sandstones in the upper layers, characteristics of the Benin formation into an alternation of both sandstone and shales characteristic of the Agbada formation, followed by an increase in shale percentage down the series. The bottom of the Benin/top of Agbada boundaries for the four wells are about 1524.0m , 1066.8m , 1981.2m and 1371.6m for Wells 1, 2, 3 and 4 respectively. The burial gradient decreases with age. Rapid subsidence episode took place between the Middle Pliocene at 3.5Ma which lasted till the Early-Pleistocene creating accommodation for the deposition of sediments with an average thickness of 1066.57m .

ACKNOWLEDGMENT

The authors are grateful to Nigerian Upstream Petroleum Regulatory Commission (NUPRC) for approving the supply of the data by SPDC for the research.

REFERENCES

Akpabio, I.O., 1997. Thermal state of the Niger Delta, Ph.D. Thesis, Rivers State University of Science and Technology, Nigeria.

Akpabio, I.O., 2009. Thermal Conductivity estimates in the Niger Delta using lithological data and geophysical well logs. The Pacific Journal of Science and Technology, 10 (1), Pp. 701 – 709.

Andrew, D.J., 1975. A numerical investigation of the thermal state of earth's mantle. Tectonophysics, 25, Pp. 177 - 186.

Benkhelil, M., Guirad, Ponsard, J.F., and Saugh, L., 1989. The Bormu-Benue trough, the Niger Delta and its offshore: Tectono-sedimentary reconstruction during the Cretaceous and Tertiary from geophysical data and geology. Compiled by C.A. Kogbe. Geology of Nigeria, Second Edition, Rock View Ltd, Pp. 277 - 310.

Chapman, D.S., Kebo, T.M., Michael, S.B., and Dane, M.P., 1984. Heat flow in the Uinta basin determined from bottom hole temperature (BHT) data. Socie. of Expl. Geoph., 49 (4), Pp. 453 - 466.

Decker, E.R., and Smithson, S.B., 1975. Heat flow and gravity interpretation across the Rio Grand rift in Southern New Mexico and West Texas. Jour of Geoph. Res., 80 (17), Pp. 2542 - 2552.

Doust, H., and Omatosla, E., 1990. The Niger Delta hydrocarbon potential of a major Tertiary Delta province, Proceedings, KNGMG Symposium Coastal lowlands, geology and geochemistry, Pp. 201 - 237.

Eliseus, O.A., Okoro, A.U., and Onuigbo, E.N., 2012. Hydrocarbon Generative Windows Determination Using Geomathematical Model: Case Study from Ogbogede Field, Niger Delta, Nigeria. Journal of Natural Sciences Research, 2 (5), Pp. 31 - 44.

Emujakporue, G.O., 2009. Subsidence and Geothermal history in the Eastern Niger Delta Basin with implications for hydrocarbons. Unpublished Ph.D. Thesis. University of Port Harcourt, Rivers State.

Erickson, A.J., Von Herzen, R.P., Sclater, J.G., Girdler, R.W., Marshall, B.V., and Hyndman, R., 1975. Geothermal measurement in deep - sea drill holes. Jour. of Geoph. Res., 80 (7), Pp. 2515 - 2528.

Evamy, B.D.J., Haremboure, P., Kamerling, W.A., Knaap, F.A., Molly, and Rowland, P.H., 1976. The hydrocarbon habitat of the Niger Delta. Expl. Bull., 252 of the Shell Petroleum Development Company of Nigeria Limited. Pp. 141 - 164.

Evamy, B.D.J., Haremboure, P., Kamerling, W.A., Knaap, F.A., Molly, and Rowland, P.H., 1978. Hydrocarbon habitat of tertiary Niger Delta. AAPG Bull., Pp. 1 - 39.

https://en.wikipedia.org/wiki/Sedimentary_basin#/media/File:Riftxsect ion.jpg, 2023.

Kaichi, S., 1984. A method of determining terrestrial heat flow in oil basinal areas. Tectonophysics, 103, Pp. 67 - 79.

Kogbe, C.A., 1989. The Cretaceous and Paleogene Sediments of Southern Nigeria, Edited by Kogbe, C. A., Geology of Nigeria, second Edition Rock View Ltd., Pp. 825 - 334.

Machens, E., 1973. The geologic history of the marginal basin along the north shore of the Gulf of Guinea, Edited by Alan, E. M. N. and G. S. France, Contained in the book titled. The Ocean Basins and Margin, vol. 1, The South Atlantic, Pp. 351 - 385.

Mckenzie, D., 1978. Some remarks on the development of sedimentary basins. Earth and Plane. Sci. Letter, 40, Pp. 25 - 32.

Middleton, M.F., 1982. The subsidence and thermal history of the Bass basins, South eastern Australia. Tectonophysics, 87, Pp. 383 - 397.

Nwaamaka, O.C., Nwachukwu, J., and Beka, F., 2015. Biostratigraphic Study of X-Well in the Alpha Field Of The Niger Delta, Nigeria. International Journal of Science Inventions Today, 4 (2), Pp. 129-139.

Odumodu, C.F.R., 2011. Subsidence and thermal history of the Calabar flank – implications for petroleum exploration. Global Journal of Geological Sciences, 7 (1), Pp. 33 - 46.

Onuoha, K.M., 1986. Basin Subsidence, Sediment decompaction and burial history modelling techniques: applicability to the Anambra basin, Proceedings of the 3rd annual conference of NAPE, 2, Pp. 6 - 17.

Onuoha, K.M., and Ofoegbu, C.O., 1988. subsidence and evolution of Nigeria's continental margin: Implications of data from Afowo - 1 well. Marine and Petroleum Geology, 5, Pp. 175 - 181.

Quike, T.T., 1980. The earth's Crust, New book of popular science. Grolier. Inc. 2, Pp. 10 - 17,

- Sass, J.N., and Samuel, E.A., 1976. Heat flow data and their relation to observed geothermal phenomena, near, Klamath falls, Oregon. *Jour. of Geoph. Res.*, 81 (6), Pp. 4868.
- Schlumberger, 1985. log interpretation principle/application, Schlumberger educational services, 3rd edition.
- Sclater, J.G.C., Jaupart and Galson, D., 1980. The heat flow through Oceanic and Continental Crust and the loss of the earth. *Reviews of Geoph. Res., and space phy.*, 98 (1), Pp. 269 - 311.
- Shannon, P.M., and Naylor N., 1989. *Petroleum Basin Studies*: London, Graham and Trotman Limited, Pp. 153-169.
- Short, K.C., and Stauble, A.J., 1967. Outline geology of the Niger Delta. *AAPG Bull.*, 51, Pp. 761 -779.
- Turcotte, D.L., and Ahern, J.L., 1977. On thermal and Subsidence and Petroleum generation in the Southern block of the Los Angeles basin, California. *Jour. of Geoph. Res.*, 84 (137), Pp. 3460 - 3464.
- Turcotte, D.L., and Schubert, G., 1973. Frictional heating of the descending hyhosphere. *Jour. of Geoph. Res.*, 78 (26), Pp. 5876 - 5885.
- Uko, E.D., 1996. Thermal Modelling of northern Niger Delta, Ph.D. Thesis, Rivers State University of Science and Technology, Nigeria.
- Uko, E.D., Alabraba, M.A., Tamunoberetonari, I., and Oki, A.O., 2021. Determination of Geothermal Gradient from Bore Hole Temperature data in Some Parts of the Eastern Niger Delta Basin. *Asian Journal of Research and Reviews in Physics*, 4 (4), Pp. 39 - 46.
- Utkelbayev, T.M., 1974. Contribution to the theory of Isostasy, 5, Pp. 276 - 277.
- Weber, K.I., and Daukoru, E., 1975. Petroleum geology of the Niger Delta, 9th World Petroleum Congress, Tokyo Proc., 2, Pp. 207 -221.
- Weber, K.J., 1971. Sedimentological aspects of all fields in Niger Delta. *Geologie Mijenbow*, 5, Pp. 539 -576.
- Weissmann, G.S., Hartley, A.J., Scuderi, L.A., Nichols, G.J., Owen, A., Wright, S., Felicia, A.L., Holland, F. and Whiteman, A., 1982. Nigeria, its petroleum geology, resources and potential, 2, Graham and Trotman.
- Wyllie, M.R.J., Gregory, A.R., and Gardner, G.H.F., 1958, An experimental investigation of factors affecting elastic wave velocities in porous media. *Geophysics*, 23, Pp. 459-493.

